AXIAL HETEROGENEITY AND FILTERED-LOAD DEPENDENCE OF PROXIMAL BICARBONATE REABSORPTION

H. BERNSTEIN, L. J. ATHERTON, AND W. M. DEEN
Department of Chemical Engineering, Massachusetts Institute of Technology, Cambridge, Massachusetts 02139

ABSTRACT A theoretical model was developed to examine the role of physical and chemical factors in the control of bicarbonate reabsorption in the renal proximal tubule. Included in the model were axial and radial variations in the concentrations of HCO_3^-, CO_2 and related chemical species in the tubule lumen and epithelial cells. Relations between these concentrations and the solute fluxes across the brush border and basolateral membranes were also included, as were reaction rate and equilibrium expressions to describe the various buffering processes in the lumen and cells. The two most critical membrane parameters, the rate constant for H^+ secretion at the brush border and the effective permeability of HCO_3^- at the basolateral membrane, were evaluated by comparing model predictions with available free-flow micropuncture data in the rat. It was found that the experimental observations could be explained only by decreasing one or both of these membrane parameters with axial position, suggesting a progressive decrease in HCO_3^- reabsorptive capacity along the tubule. For single nephron filtered loads of HCO_3^- up to about 1,400 pmol/min, absolute bicarbonate reabsorption was predicted to increase nearly in proportion to filtered load, whereas it was calculated to be relatively constant at higher filtered loads, irrespective of how filtered load was assumed to be varied. These predictions are in excellent agreement with most of the available micropuncture data in rats, as is the prediction that HCO_3^- reabsorption should change in parallel with CO_2 partial pressure in the filtrate, at a given filtered load of HCO_3^-. Certain discrepancies between the model predictions and experimental observations are evident at very high filtered loads, and the implications of these are discussed in terms of possible adaptive responses of the tubule.

INTRODUCTION

Bicarbonate is the principal buffer in blood, and the maintenance of appropriate levels of bicarbonate in plasma is therefore a critical element in the control of plasma pH. Under normal conditions this control system requires that relatively little bicarbonate be excreted in urine. The normal role of the renal proximal tubule is to reabsorb a large fraction of the bicarbonate present in glomerular filtrate (typically 80–90%), and return it to the circulation via the peritubular capillaries. When glomerular filtration rate is increased, so is the rate of proximal bicarbonate reabsorption. This prevents excessive excretion of bicarbonate in urine, which could lead to acidosis.

The handling of bicarbonate and carbon dioxide by the proximal tubule has been examined extensively in vivo using free-flow micropuncture and in situ microperfusion techniques, and in vitro by perfusion of isolated tubule segments, as reviewed by Warnock and Rector (1). The principal transport steps and chemical reactions that are thought to be involved in the reabsorption of bicarbonate and acidification of tubule fluid in this nephron segment are depicted in Fig. 1. The primary event is believed to be secretion of H^+ from epithelial cell to tubule lumen (closely coupled to Na^+ reabsorption), which titrates luminal HCO_3^- to form CO_2. Although not shown, HCO_3^- titration also leads to the formation of small amounts of H_2CO_3. These substances (primarily CO_2) are thought to diffuse into the cell, allowing generation of new intracellular HCO_3^-. This new HCO_3^- passes across the basolateral membrane into the peritubular interstitium, where it gains ready access to the peritubular microcirculation.[1] The net effect of this cycle is the movement of HCO_3^- from tubule lumen to blood. Of importance is that the predominant pathway for interconversion of CO_2 and HCO_3^- is enzymatic, involving carbonic anhydrase (C.A.) within the cell and at the luminal surface of the brush border membrane.

Address all correspondence to Professor William M. Deen, Department of Chemical Engineering, 66-509, Massachusetts Institute of Technology, Cambridge, MA 02139

[1]The movement of a bicarbonate ion from the proximal epithelial cell to the peritubular interstitium is equivalent to the transport of one molecule of carbon dioxide together with a hydroxyl ion. In addition, because of the rapid equilibrium involved in the dissociation of water, transport of OH^- in one direction is equivalent to transport of H^+ in the other. Although we have chosen to view HCO_3^- as the species transported across the basolateral membrane, the identity of the transported species is not yet well established.

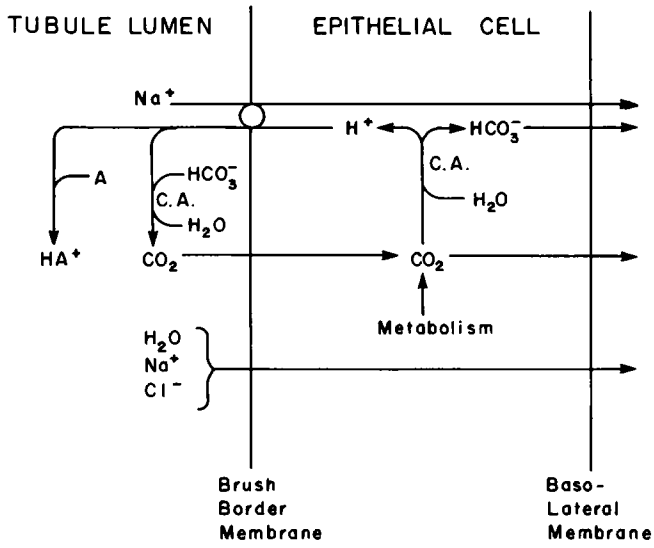

FIGURE 1 Schematic diagram illustrating the mechanism of HCO_3^- reabsorption in the renal proximal tubule. Carbonic anhydrase is denoted by C.A. and nonbicarbonate buffers (e.g. HPO_4^-) by A.

In addition to titrating luminal HCO_3^-, secreted H^+ may react with various non-bicarbonate buffers that appear in tubule fluid, denoted collectively by "A" in Fig. 1. The most important of these is divalent phosphate (HPO_4^-). Concurrent with the various transport and reaction steps already described is the reabsorption of large amounts of H_2O, Na^+, and Cl^-. It should be noted that HCO_3^- is reabsorbed more rapidly than water, so that the luminal HCO_3^- concentration declines with distance along the proximal tubule. The resulting transepithelial concentration gradient favors HCO_3^- "backleak" from interstitium to lumen, presumably by diffusion through intercellular channels.

Many of the quantitative aspects of the bicarbonate reabsorption process remain to be elucidated. To examine some of the implications of currently accepted hypotheses, Wang and Deen (2) developed a model which focuses exclusively on the main HCO_3^-/CO_2 cycle described above. Radial and axial concentration profiles for CO_2, HCO_3^-, and H_2CO_3 in the tubule lumen and epithelium were determined using conservation of mass equations applied to both regions, assuming membrane transport of these species to be passive. Interstitial concentrations and intracellular pH were specified as constants. The rate of secretion of H^+ was assumed to equal the intracellular rate of HCO_3^- generation and was calculated from the HCO_3^- mass balance in the cell. This assumption and the specification of intracellular pH as an input parameter eliminated the need to relate the rate of H^+ secretion to luminal and intracellular pH.

Several factors not included in the model of Wang and Deen (2) limit its applicability to the earliest segment of the proximal tubule. First, nonbicarbonate buffers were neglected. This approximation is appropriate early in the proximal tubule, but should become increasingly inadequate in later portions as the concentration of HCO_3^- declines relative to that of other buffers. Second, paracellular backleak of HCO_3^- was not considered, and this too may become significant when luminal HCO_3^- concentrations are low. Third, no provision was made for a direct effect of luminal acidity on H^+ secretion rate or intracellular pH. Recent micropuncture data in the rat (3–5) demonstrate that bicarbonate reabsorption rate (H^+ secretion rate) declines markedly along the proximal convoluted tubule as luminal HCO_3^- concentration and pH decrease.

The objective of the study reported here was to incorporate these additional factors into a theoretical model for proximal bicarbonate reabsorption. By obtaining more realistic descriptions of pH and concentration variations along the length of the proximal tubule, we have been able to examine the response to variations in the rate of bicarbonate delivery to the tubule ("filtered load"), which could not be done with our previous model (2). Many of the factors considered here were included also in a model presented very recently by Alpern and Rector (6), but using a less mechanistic approach. Whereas those authors calculated bicarbonate reabsorption rates using a series of empirical correlations derived largely from microperfusion data, our approach has been to relate reabsorption rates to specific physico-chemical quantities such as membrane permeabilities, diffusion coefficients, and reaction rate and equilibrium constants. Many of the physical constants in our model could be estimated independently, although certain critical membrane parameters had to be obtained by fitting our results to micropuncture data on bicarbonate reabsorption in the rat. Our predictions of pH variations and bicarbonate reabsorption rates are compared, where possible, to available micropuncture data.

MODEL FORMULATION

General Considerations

As shown in Fig. 2, the proximal tubule epithelium consists of a single layer of cuboidal cells, and was modeled as a circular tube of inner radius r_1 (approximately 15 μm in the rat) and outer radius r_2 (25 μm). Because of secretion, reabsorption, and chemical reactions, the steady-state concentrations of the various chemical species depend on both radial position (r) and axial position (z), the latter being measured from Bowman's capsule. The analysis involved detailed consideration of two regions, the tubule lumen ($0 \leqq r < r_1$, concentration C_i for species i) and the intracellular fluid ($r_1 < r < r_2$, concentration C_{ic}). On the length scale of interest, cell membrane thicknesses are of course negligible. Interstitial concentrations (C_{ib}) were assumed to equal those in peritubular capillary plasma, and were specified in most cases as input parameters that were independent of position along the tubule. Six chemical species were considered, identified by the following sub-

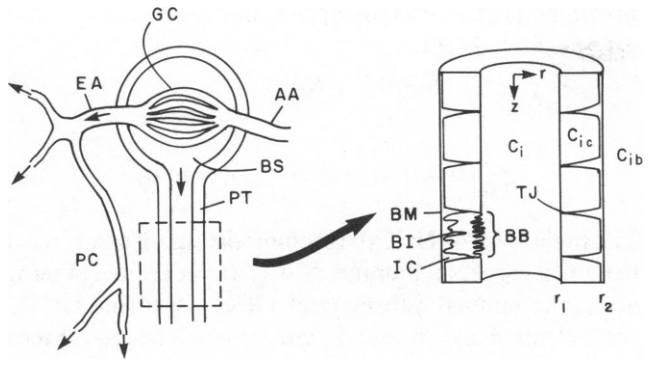

FIGURE 2 Anatomical structures and model geometry. *Left:* AA, afferent arteriole; GC, glomerular capillaries; EA, efferent arteriole; BS, Bowman's space; PT, proximal tubule; PC, peritubular capillaries. *Right:* BM, basement membrane; BI, basal infoldings; IC, intercellular channel; TJ, tight junction; BB, brush border.

script notation:

i = 1:	CO_2	4:	H^+
2:	HCO_3^-	5:	$H_2PO_4^-$
3:	H_2CO_3	6:	HPO_4^-

In the pH range of the proximal convoluted tubule (~6.8–7.4) the amounts of CO_3^-, H_3PO_4, and PO_4^{-3} are negligible. Carbonic acid (H_2CO_3) is also present in relatively small amounts, but was included because of its role as a reaction intermediate (see below).

The various chemical reactions will be referred to as homogeneous if they occur throughout a compartment, and heterogeneous if they are confined to a membrane surface; the former appear as source terms in the species conservation equations, the latter in boundary conditions. Forward and reverse rate constants for reaction j are denoted by k_j and k_{-j}, respectively, with the corresponding equilibrium constant defined as $K_j = k_{1j}/k_{-j}$. As discussed previously (2), the interconversion of CO_2 and HCO_3^- may be described by three reactions

$$CO_2 + H_2O \underset{k_{-1}}{\overset{k_1}{\rightleftharpoons}} H_2CO_3 \qquad \text{(Reaction 1)}$$

$$H_2CO_3 \underset{k_{-2}}{\overset{k_2}{\rightleftharpoons}} H^+ + HCO_3^- \qquad \text{(Reaction 2)}$$

$$CO_2 + H_2O \underset{\text{C.A.}}{\overset{k_3}{\underset{k_{-3}}{\rightleftharpoons}}} H^+ + HCO_3^- \qquad \text{(Reaction 3)}$$

Reactions 1 and 2 represent the nonenzymatic pathway, whereas reaction 3 is catalyzed by carbonic anhydrase. All three were considered to occur as homogeneous reactions within the cell, with reaction 3 being dominant (except during carbonic anhydrase inhibition) because of its much higher rate constants. Carbonic anhydrase appears to be present not only within the cell but at the luminal surface of the brush border membrane ($r = r_1$), so that in the lumen reaction 3 was treated as heterogeneous. While not catalyzed by a membrane-bound enzyme, reaction 2 between secreted H^+ and luminal HCO_3^- is sufficiently fast that it should reach equilibrium within a few angstroms of the membrane surface (2), so that it too was treated as heterogeneous. Similar reasoning applies to the rapid protonation of HPO_4^- in the tubule lumen

$$H_2PO_4^- \underset{k_{-4}}{\overset{k_4}{\rightleftharpoons}} H^+ + HPO_4^- \qquad \text{(Reaction 4)}$$

Thus, the only homogeneous reaction considered in the lumen was the uncatalyzed hydration of CO_2, reaction 1. Metabolic formation of CO_2, neglected previously (2), was described as a zero-order, homogeneous reaction within the epithelial cell.

An important assumption was that intracellular pH is independent of position within a given cell. Although not rigorously justifiable, this assumption is made plausible by the high mobility of H^+ and the probable facilitation of H^+ transport by various intracellular buffers (7). Accordingly, a detailed description of intracellular buffering processes, including the intracellular handling of phosphates, was not attempted. As in our previous model (2), the net rate of formation of H^+ within the cells was equated with that of HCO_3^- (see reactions 2 and 3), and all of this H^+ was assumed to be secreted into the lumen. However, a specific relationship between intracellular H^+ concentration and secretion rate was postulated in the present model (see Eq. 8), and intracellular pH calculated as a function of position along the tubule (z), rather than specified as a position-independent input parameter.

Transport of the chemical species modeled, other than phosphates, was assumed to be passive. Diffusion of CO_2 and H_2CO_3 was assumed to be transcellular, while parallel transcellular and paracellular pathways were included for HCO_3^-. The rate of phosphate removal from the lumen was taken to be constant, with equal amounts of phosphate being reabsorbed in the monovalent ($H_2PO_4^-$) and divalent (HPO_4^-) forms. If reabsorbed phosphate was assumed to be exclusively monovalent or divalent, then the cumulative bicarbonate reabsorption rate up to the end of the proximal convoluted tubule was calculated to change by <1%.

Intracellular Transport

Transport within the cells was assumed to occur only in the radial direction. The differential equations used to express conservation of mass for CO_2, HCO_3^- and H_2CO_3 were as given previously (2), except for the addition of a homogeneous reaction term (M_1) representing metabolic formation of CO_2. Reaction 2 is very fast, and with normal carbonic anhydrase activity, so is reaction 3. A good approximation to the intracellular concentration profiles

could therefore be obtained by assuming local equilibrium

$$C_{2c} = K_3 C_{1c}/C_{4c} \quad (1)$$

$$C_{3c} = K_1 C_{1c}. \quad (2)$$

Integration of the conservation equations then yielded the following result for the intracellular CO_2 concentration

$$C_{1c}(\xi) = \frac{-M_1 r_1^2 \xi^2}{4[D_{1c} + (D_{2c}K_3/C_{4c}) + D_{3c}K_1]} + T_1 \ln \xi + T_2, \quad (3)$$

where $\xi = r/r_1$ is a dimensionless radial coordinate and D_{ic} is the intracellular diffusion coefficient of substance i. The integration constants T_1 and T_2 were chosen to satisfy continuity of the flux of "total CO_2" at both membranes (2). Details of analogous derivations were given by Wang and Deen (2) and Maddox et al. (3).

Luminal Transport

According to our assumption that both of the buffer pairs are in equilibrium (i.e., that reactions 2 and 4 are fast) two of the six luminal concentrations may be determined from the others. Thus, only four conservation equations are needed to determine the radial and axial variations in the luminal concentrations. We chose to write the conservation equations in terms of CO_2, HCO_3^-, H_2CO_3, and total phosphate ($H_2PO_4^-$ + HPO_4^-). As justified previously (2), axial diffusion was neglected and radial concentration variations were approximated using second order polynomials in ξ. The latter assumption allowed the partial differential conservation equations to be integrated analytically in the radial direction, reducing them to ordinary differential equations.

The conservation equations are written most conveniently in terms of bulk or flow-average concentrations, $\bar{C}_i(\eta)$, where $\eta = z/r_1$ is dimensionless axial position

$$\bar{C}_i(\eta) = \frac{\int_0^1 C_i(\eta, \xi)\, v_z\, \xi\, d\xi}{\int_0^1 v_z\, \xi\, d\xi}. \quad (4)$$

Assuming the fluid reabsorption rate in the tubule to be approximately constant, yielding a constant radial velocity at the luminal membrane surface (v_m), the axial velocity (v_z) is given by (8)

$$v_z = 2(v_0 - 2v_m\eta)(1 - \xi^2). \quad (5)$$

In Eq. 5 v_0 is the initial mean axial velocity (at $\eta = 0$), given by $SNGFR/\pi r_1^2$, where $SNGFR$ is the single nephron glomerular filtration rate.

The conservation equations for CO_2 and H_2CO_3 in the tubule lumen are as given previously (2). The equations governing HCO_3^- and total phosphate are

$$\frac{1}{2}\frac{d}{d\eta}[\bar{C}_2(v_0 - 2v_m\eta)] = -N_2|_{\xi=1} + P_{2L}(C_{2b} - C_2|_{\xi=1}) \quad (6)$$

$$\frac{1}{2}\frac{d}{d\eta}[(\bar{C}_5 + \bar{C}_6)(v_0 - 2v_m\eta)] = -N_{pm}. \quad (7)$$

The radial flux of HCO_3^- reaching the luminal surface of the brush border membrane, $N_2|_{\xi=1}$, was evaluated in terms of v_m, the luminal diffusivity of HCO_3^-, and the HCO_3^- concentration and its radial gradient (2). The second term on the right hand side of Eq. 6 represents paracellular backleak of HCO_3^-, with the paracellular permeability denoted by P_{2L}. The flux of total phosphate out of the tubule lumen (based on the area of the cylinder defined by $r = r_1$) is denoted by N_{pm}. The reader is referred elsewhere (2) for the additional relationships required to calculate radial concentration gradients, fluxes, and reaction rates in the tubule lumen.

Membrane Transport and H^+ Balance

H^+ transport from proximal epithelial cell to lumen is widely believed to proceed against an unfavorable pH gradient, but the precise relationship between H^+ secretion rate in vivo and luminal and intracellular pH values has not been established. We employed an expression analogous to that suggested by Alpern et al. (9)

$$-N_{4m}|_{\xi=1} = \beta(\alpha C_{4c} - C_4|_{\xi=1}), \quad (8)$$

where β and α are constants. Setting $\alpha > 1$ allows the H^+ secretory flux, $-N_{4m}|_{\xi=1}$, to be positive despite an unfavorable pH gradient. For H^+ secretion to cease when intracellular pH exceeds luminal pH by one unit, $\alpha = 10$ is required. According to the view that there is a 1:1 passive exchange of Na^+ for H^+ at the brush border membrane, driven by the low intracellular concentration of Na^+, α is equivalent to the extracellular-to-intracellular Na^+ concentration ratio (9).

Based on the assumption that equal amounts of H^+ and HCO_3^- are generated by intracellular reactions, and that all of this H^+ is secreted, the steady-state flux of H^+ could also be related directly to the rate of HCO_3^- efflux from the cells

$$N_{4m}|_{\xi=1} = N_{2m}|_{\xi=1} - (r_2/r_1)\, N_{2m}|_{\xi=r_2/r_1}. \quad (9)$$

Eq. 9 neglects the formation of H^+ from cellular metabolism and from any intracellular buffering associated with the transport of other substances (e.g. phosphates). An additional relationship involving the flux of H^+ was obtained from the assumption that all secreted H^+ is consumed in titrating luminal buffers (HCO_3^- and HPO_4^-)

$$N_{4m}|_{\xi=1} = \phi_2^{(2)} + (k_3' C_1 - k_{-3}' C_2 C_4) - N_6|_{\xi=1} + \frac{N_{pm}}{2}. \quad (10)$$

The first two terms on the right hand side represent the rate of formation of HCO_3^- per unit area at the luminal membrane surface, with $\phi_2^{(2)}$ and the quantity in parentheses giving the contributions from reactions 2 and 3, respectively. The remaining terms give the rate of formation of $HPO_4^=$; the factor ½ in the last term on the right is based on the assumption that one-half of the reabsorbed phosphate is in the divalent form. Details of the derivation of an expression analogous to Eq. 10 have been presented previously (2).

Membrane transport of CO_2, HCO_3^-, and H_2CO_3 was assumed to be passive (2). In particular, the flux of HCO_3^- (or HCO_3^- equivalents) across the basolateral membrane was described by

$$N_{2m}|_{\xi=r_2/r_1} = \frac{P_2(r_2)\,\Delta\psi[C_{2c}|_{\xi=r_2/r_1} - C_{2b}e^{-\Delta\psi}]}{1 - e^{-\Delta\psi}}, \quad (11)$$

where $P_2(r_2)$ is the effective HCO_3^- permeability and $\Delta\psi$ is the dimensionless potential difference across the membrane (peritubular interstitium minus cell). $\Delta\psi$ is the actual potential difference divided by RT/F, the product of the gas constant and the absolute temperature divided by Faraday's constant (RT/F = 26.7 mV at 37°C). Eq. 11 was derived using a constant field approximation (10). As already mentioned, the flux of total phosphate at the brush border (N_{pm}) was taken to be independent of axial position along the tubule.

TABLE I
REFERENCE VALUES FOR MODEL PARAMETERS

Diffusivities (cm^2/s)		
$D_1 = 2.30 \times 10^{-5}$	$D_5 = 1.27 \times 10^{-5}$	$D_{1C} = 1.02 \times 10^{-5}$
$D_2 = 1.57 \times 10^{-5}$	$D_6 = 1.01 \times 10^{-5}$	$D_{2C} = 5.36 \times 10^{-6}$
$D_3 = 1.57 \times 10^{-5}$	$D_7 = 1.98 \times 10^{-5}$	$D_{3C} = 5.36 \times 10^{-6}$
Permeabilities (cm/s)		
$P_1(r_1) = 5.4$	$P_2(r_1) = 0$	$P_3(r_1) = 3.6 \times 10^{-2}$
$P_1(r_2) = 3.0$	$P_{2L} = 2.8 \times 10^{-5}$	$P_3(r_2) = 2.0 \times 10^{-2}$
Equilibrium and Reaction Rate Constants		
$K_1 = 2.50 \times 10^{-3}$		$K_4 = 1.59 \times 10^{-10}$ mol/cm³
$K_2 = 3.18 \times 10^{-7}$ mol/cm³		$k_1 = 0.08\ s^{-1}$
$K_3 = 7.94 \times 10^{-10}$ mol/cm³		$k_3' = 1.0$ cm/s
Solute Concentrations (mol/cm³)		
$C_1(0) = 1.65 \times 10^{-6}$		$C_{1b} = 1.65 \times 10^{-6}$
$C_2(0) = 3.08 \times 10^{-5}$		$C_{2b} = 2.93 \times 10^{-5}$
$C_3(0) = 4.12 \times 10^{-9}$		$C_{3b} = 4.12 \times 10^{-9}$
$C_5(0) + C_6(0) = 2.3 \times 10^{-6}$		
Other Quantities		
$r_1 = 1.5 \times 10^{-3}$ cm		$\Delta\psi = 2.62$
$r_2 = 2.5 \times 10^{-3}$ cm		$\alpha = 10$
$v_0 = 9.62 \times 10^{-2}$ cm/s		$\beta_0 = 26$ cm/s
$v_m = 6.80 \times 10^{-5}$ cm/s		$P_0 = 1.44 \times 10^{-4}$ cm/s
$N_{pm} = 2.0 \times 10^{-10}$ mol cm^{-2}s^{-1}		$\delta = 0.574$ mm^{-1}

Computational Procedure

To evaluate the various fluxes and satisfy the boundary conditions at $\xi = 1$ and $\xi = r_2/r_1$, a set of 20 nonlinear algebraic equations had to be solved at each axial position, and this was done using the Newton-Raphson method. To determine C_i at new axial positions, the luminal conservation equations (e.g., Eqs. 6 and 7) were integrated using a fourth-order Runge-Kutta routine. Initial values of the bulk concentrations, $C_i(0)$, were provided by specifying the composition of the glomerular filtrate.

RESULTS

Most of the results to be presented are based on the parameter values summarized in Table I. Diffusivities of CO_2, HCO_3, and H_2CO_3 in the tubule lumen and cell cytoplasm were derived from values reported by Gros and Moll (11) for water and concentrated protein solutions, respectively, at 22°C. The reported values were increased by a factor of 1.34 to correct them to 37°C; this correction factor was obtained by assuming that $D_i\mu/T$ is constant, where μ is the viscosity of water. Luminal diffusivities of $H_2PO_4^-$ and $HPO_4^=$ (7) were also corrected to 37°C. Estimates of the cell membrane permeabilities for CO_2 and H_2CO_3 were obtained from values reported for red blood cells or lipid bilayers, adjusted upward to account for the increases in surface area due to the brush border microvilli and basal infoldings, as discussed previously (2). The paracellular permeability of HCO_3^-, P_{2L}, is based on the transepithelial permeability coefficient in the rat reported by Alpern et al. (12). In evaluating P_{2L} in this manner, we have chosen to neglect any transcellular contribution to the "passive" flux of HCO_3^-, and have set $P_2(r_1) = 0$. As shown previously (2), nonzero values of $P_2(r_1)$ lead to HCO_3^- diffusion from the cell to the tubule lumen, requiring higher values of $P_2(r_2)$ to effect a given net rate of HCO_3^- reabsorption. Calculations with the present model confirm that, other than its effect on the estimated value of $P_2(r_2)$ (determined as described below), the value chosen for $P_2(r_1)$ is of little importance.

The reaction rate and equilibrium constants were obtained for the most part directly from the literature (7, 13). The rate constant k_3' for reaction 3 at the luminal surface of the brush border membrane was chosen to insure that greater than 99% of the HCO_3^- titrated at this surface was converted to CO_2, consistent with the concept of a fast, heterogeneous reaction catalyzed by carbonic anhydrase (2).

Bulk concentrations of CO_2 and H_2CO_3 in Bowman's space ($C_1[0]$ and $C_3[0]$) are based on the finding that the partial pressure of CO_2 (PCO_2) equals 55 mm Hg at this location in the rat (3). Although PCO_2 was found to exceed this value by 0–4 mm Hg at various sites in the superficial cortical microcirculation (3), we have generally not

attempted to include spatial variations in the boundary conditions at $r = r_2$, and have instead assumed that $PCO_2 = 55$ mm Hg in the peritubular blood and interstitial fluid. Thus, $C_{1b} = C_1(0)$ and $C_{3b} = C_3(0)$. The HCO_3^- concentration in Bowman's space ($C_2[0]$) is the mean arterial value measured in a study using Munich-Wistar rats (4), multiplied by a factor of 1.16 (14). Assuming a Donnan factor of 1.05, the peritubular HCO_3^- concentration is given by $C_{2b} = C_2(0)/1.05$. The concentration of total phosphate in Bowman's space ($C_5[0] + C_6[0]$) was derived from measurements of total phosphate in systemic arterial plasma in the rat (15).

The luminal velocities v_0 and v_m are based on a single nephron glomerular filtration rate (*SNGFR*) of 40.8 nl/min (3) and a water reabsorption rate of 19.2 nl/min (see Eq. 15), for a tubule with a luminal radius (r_l) of 15 μm and a length of 5 mm. The rate of total phosphate reabsorption (N_{pm}) is based on the observation that ~60% of filtered phosphate is reabsorbed in the rat proximal tubule when *SNGFR* $\simeq$ 30 nl/min (15). The dimensionless transmembrane potential difference ($\Delta\psi$) corresponds to an intracellular potential of -70 mV relative to blood. The physical interpretation of the parameter α has already been discussed in connection with Eq. 8; $\alpha = 10$ was chosen to approximate the extracellular-to-intracellular ratio of Na^+ concentrations.

By far the most critical membrane parameters are the HCO_3^- permeability at the basal side of the cell, $P_2(r_2)$, and the proton secretion rate constant, β. These were estimated by fitting the calculated rates of bicarbonate reabsorption to those measured by Maddox and Gennari (4) using free-flow micropuncture in Munich-Wistar rats. Based on an extensive set of measurements in animals with normal plasma pH and HCO_3^- concentration, those authors reported fractional bicarbonate reabsorption (F_B) as a function of the filtered load of bicarbonate ($\Lambda = SNGFR \cdot C_2[0]$) and distance ($z$) along the tubule from Bowman's space. The data include values of z from <1 mm to ~5 mm, and Λ from about 400 to 2,400 pmol/min (the base case in Table I corresponds to $\Lambda = 1{,}257$ pmol/min). In these experiments Λ varied primarily with *SNGFR*, $C_2(0)$ being nearly constant. At a given Λ, HCO_3^- was reabsorbed more and more slowly as z increased; at a given z, F_B varied inversely with Λ. To be consistent with both of these effects, and noting the requirement that $F_B = 0$ at $z = 0$, we correlated the data using an expression of the form

$$F_B = \frac{1 - \exp(-a_1 z)}{a_2 + a_3 \Lambda + a_4 \Lambda^2}. \quad (12)$$

The constants $a_1 - a_4$ were chosen to minimize the mean square error between Eq. 12 and the data. Using values of 0.712, 0.974, 1.09×10^{-4} and 3.70×10^{-8} (where z is in mm and Λ is in pmol/min), respectively, a very adequate fit was obtained (RMS error = 0.08). It may be noted that Eq. 12 is highly consistent not only with the data of Maddox and Gennari (3, 4) but with the results of several other micropuncture studies in the rat, under normal acid-base conditions (5, 16–18).[2] The mean values of Λ in these other studies ranged from about 600 to 1,500 pmol/min, depending on the extracellular fluid volume and on other experimental maneuvers used to alter renal hemodynamics. Accordingly, we have employed Eq. 12 to summarize all experimental findings on the variation of F_B with z and Λ under normal acid-base conditions, where Λ varies primarily with *SNGFR*.

Fig. 3 presents a comparison of measured fractional rates of bicarbonate reabsorption along the proximal tubule with those calculated using several variations of our model. Fractional bicarbonate reabsorption is obtained from $F_B = R_B/\Lambda$, where R_B is the absolute rate of bicarbonate reabsorption up to the position indicated (cumulative). Curve *A* corresponds to the model described previously by Wang and Deen (2), while curves *B–D* were obtained by the successive addition of several new features to the basic model: variable H^+ secretion kinetics and intracellular pH (curve *B*), paracellular backleak of HCO_3^- (curve *C*), and phosphates and metabolic CO_2 (curve *D*). In each case the parameters $P_2(r_2)$ and β were adjusted to match the typical experimental finding of $F_B = 0.83$ at $z = 5$ mm. It can be seen that even for the most complete of these models (curve *D*), $F_B(z)$ is predicted to be almost linear, implying a nearly constant rate of HCO_3^- reabsorption along the tubule. This is in marked contrast with the experimental findings depicted by curve *F* (based on Eq. 12). It is noteworthy that, to attribute the nonlinearity of the experimental values of $F_B(z)$ to HCO_3^- backleak, the paracellular HCO_3^- permeability (P_{2L}) would have to be some twenty times the value given in Table I.

To bring the model calculations into full agreement with the experimental curve for $F_B(z)$, it was necessary to introduce axial variations in the HCO_3^- permeability at the basolateral membrane ($P_2[r_2]$), in the H^+ secretion rate parameter (β), or in both. Simultaneously decreasing both of these parameters with distance along the tubule provided the best agreement. The functional forms chosen were

$$P_2(r_2) = P_0 e^{-\delta z} \quad (13)$$

$$\beta = \beta_0 e^{-\delta z}. \quad (14)$$

The values of P_0 and β_0 determine the initial rate of bicarbonate reabsorption, whereas the value of δ is critical in establishing the shape of the fractional reabsorption curve. Using the values of these parameters given in Table I we obtained curve *E* in Fig. 3, which is indistinguishable from the experimental results. The value of δ employed corresponds to β and $P_2(r_2)$ values at $z = 5$ mm that are ~6% of their initial levels.

[2]For samples described as "late proximal," but where the tubule length up to the point of micropuncture was not reported, we have assumed a typical length of 5 mm.

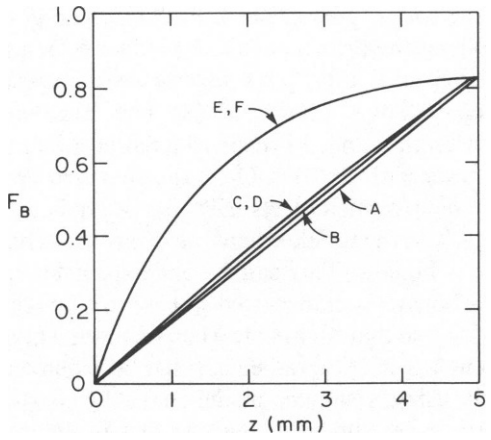

FIGURE 3 Fractional bicarbonate reabsorption (F_B) as a function of position (z) along the proximal tubule. Curve A is based on the model of Wang and Deen (2), while curve E represents the complete present model; curves B–D are based on various intermediate formulations, as described in the text. Curve F represents experimental data of Maddox and Gennari (4) in the rat. In each of these simulations (A–E) the membrane parameters for H^+ and HCO_3^- transport have been adjusted to match the observed value of F_B at z = 5 mm. Other inputs are as given in Table I.

The specific effects of adding phosphates and bicarbonate backleak to the model are better illustrated in Fig. 4. Curve E in Fig. 4 is identical to that in Fig. 3, and represents the most complete model, including the axial variations in membrane parameters described by Eqs. 13 and 14. Curve E' in Fig. 4 represents the effect of removing phosphates and metabolic CO_2 formation from the model, while maintaining the membrane parameters at the values in Table I. Slightly higher values of F_B are obtained in curve E' than curve E, because in the former case there is no HPO_4^- to compete with HCO_3^- for secreted H^+.

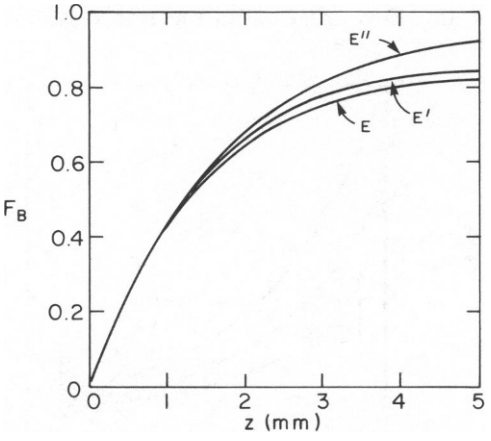

FIGURE 4 Fractional bicarbonate reabsorption (F_B) as a function of position (z) along the proximal tubule. Curve E is the same as in Fig. 3, and represents the most complete model. Curves E' and E'' are based on the complete model except for nonbicarbonate buffers, and the complete model except for nonbicarbonate buffers and intercellular bicarbonate backleak, respectively. All three cases are based on the same parameters for transcellular H^+ and HCO_3^- transport.

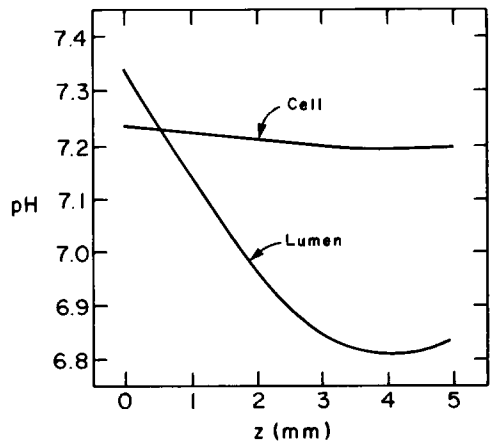

FIGURE 5 Luminal and intracellular pH as a function of axial position along the tubule, calculated for the baseline conditions given in Table I.

Accordingly, all of the secreted H^+ is available to effect HCO_3^- reabsorption in the simulation denoted by curve E', and HCO_3^- reabsorption rates are slightly greater. The presence or absence of metabolic CO_2 was found to have a negligible effect on F_B (or R_B). The simulation represented by curve E'' in Fig. 4 differs from that of curve E' in that HCO_3^- backleak has also been eliminated (P_{2L} = 0 in this case). A significant enhancement of net bicarbonate reabsorption is predicted when backleak no longer occurs, especially at relatively late positions along the tubule. It may be concluded from Fig. 4 that bicarbonate backleak noticeably affects rates of bicarbonate reabsorption in the proximal tubule, even though it fails to explain the very large axial variations in bicarbonate reabsorption rate seen in micropuncture studies in the rat.

Fig. 5 shows the changes in luminal and intracellular pH with position along the tubule calculated using parameter values corresponding to curve E in Fig. 3, the complete model. We will subsequently refer to this parameter set as the baseline case. Intracellular pH is predicted to be higher than luminal pH everywhere but in the first 0.5 mm. The decrease in luminal pH causes a parallel, but much smaller decrease in intracellular pH. As luminal pH decreases from 7.34 to 6.85, intracellular pH decreases from 7.24 to 7.20. Note that luminal pH is predicted to increase slightly at the end of the accessible proximal tubule. This is a

TABLE II
ALTERNATE CHOICES OF BICARBONATE PERMEABILITY AND HYDROGEN SECRETION PARAMETERS

	β_0	P_0	δ	Calculated pH_c
	cm/s	*cm/s*	mm^{-1}	
Baseline	26	1.44×10^{-4}	0.574	7.24–7.20
High pH_c	50	8.00×10^{-5}	0.574	7.48–7.42
Low pH_c	15	2.48×10^{-4}	0.574	7.02–7.00

pH_c = intracellular pH

consequence of an increasing luminal bicarbonate concentration, which is itself a reflection of a very small hydrogen ion secretion rate at this location. The luminal bicarbonate concentration can increase even while bicarbonate is being reabsorbed, provided that fluid reabsorption is more rapid. The slight increase in luminal pH is predicted to induce a very small accompanying increase in intracellular pH as well.

Two other combinations of β and $P_2(r_2)$ which yield fractional bicarbonate reabsorption curves virtually identical to curve E in Fig. 3 are given in Table II. Notice that δ is the same for all three cases so that the shape of the fractional bicarbonate reabsorption curves is the same. The axial variation of luminal pH for the two alternate combinations is essentially the same as the baseline case. However, the values of predicted intracellular pH are significantly different. For the combination in which β_0 is higher than the baseline β_0 and P_0 lower than the baseline value, the predicted intracellular pH(pH_c) is ~7.4, uniformly higher than the baseline case. For the combination that has a lower β_0 and higher P_0 than in the base case, the pH_c is uniformly lower, ~7.0. These results can be understood by considering the effect that β and $P_2(r_2)$ have on the hydrogen secretion rate at the brush border ($r = r_1$) and the bicarbonate flux at the basolateral membrane (r_2). From Eq. 11, the bicarbonate flux at r_2 is equal to the permeability at r_2 multiplied by the electrochemical driving force. For a smaller permeability, the driving force must be larger to achieve the same flux. To achieve a larger driving force, intracellular HCO_3^- is higher and since intracellular CO_2 is essentially constant for all the cases, higher intracellular pH is favored as well. Similarly, from Eq. 8, the hydrogen secretion rate equals the rate constant (β) multiplied by the appropriate driving force. If β is larger than the baseline β, a smaller driving force is necessary to achieve the same hydrogen ion secretion rate. This condition favors a smaller intracellular hydrogen ion concentration (larger pH_c). Therefore, a simultaneous increase in β and decrease in $P_2(r_2)$ tends to produce a higher intracellular pH in order to maintain the same bicarbonate flux. The same argument holds in reverse when β is decreased and $P_2(r_2)$ increased above baseline levels.

The results just described suggest that while unique combinations of β and $P_2(r_2)$ cannot be deduced from bicarbonate reabsorption data alone, measurements of intracellular pH in the rat proximal epithelium, under conditions similar to those existing during the reabsorption measurements, might make this possible. Using pH-sensitive microelectrodes, an intracellular pH value of 7.16 has been reported recently for the rat proximal convoluted tubule perfused in vivo (19), suggesting that the parameters for our baseline case are more representative of physiological conditions than are the other cases considered. Additional information, of a less direct nature, is available from reported values of the transepithelial difference in the partial pressure of CO_2, ΔPCO_2. Fig. 6 shows ΔPCO_2 along the proximal tubule predicted for the three combinations of β and $P_2(r_2)$, together with experimental results reported by Maddox et al. (3). The shaded areas are derived from the range of reported axial positions and the average transepithelial ΔPCO_2 ± the standard error. For each of the parameter sets ΔPCO_2 is predicted to be highest early in the tubule where the bicarbonate reabsorption rate is highest. This can be understood by recalling that bicarbonate is transported out of the lumen in the form of CO_2, so that higher bicarbonate reabsorption rates result from larger CO_2 gradients. It has been demonstrated previously using a simpler model that ΔPCO_2 should be very nearly proportional to the flux of CO_2 at the brush border (3). In the same study, ΔPCO_2 was also predicted to increase as the intracellular pH decreases. The three combinations of β_0, P_0, and δ in Table II have been chosen to give the same bicarbonate reabsorption rates and hence the same CO_2 fluxes across the luminal membrane. However, because the intracellular pH values predicted are very different for each combination, they lead to significantly different ΔPCO_2 profiles along the tubule. The agreement between the experimental ΔPCO_2 values and those given by the baseline case, both early and late in the tubule, lends further support to the choices for β_0, P_0, and δ given in Table I.

The results presented thus far are based on the assumption that the pH and the concentrations of CO_2 and HCO_3^- in peritubular interstitial fluid are uniform along the proximal tubule, and equivalent to those of afferent arteriolar plasma. To assess the effect of the assumed peritubular conditions, we calculated F_B again using parameters from Table I, with the exception that peritubular PCO_2 and HCO_3^- concentration were varied linearly along the tubule. For these calculations peritubular concentrations were based on the observation that the late proximal tubule segments are often adjacent to the star vessel (efferent

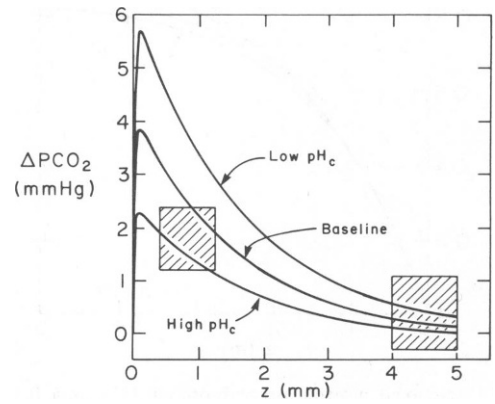

FIGURE 6 Transepithelial difference in CO_2 partial pressure (lumen minus peritubular fluid) as a function of position along the tubule. The solid curves are model predictions based on the three sets of membrane parameters given in Table II. The shaded areas are based on the PCO_2 measurements of Maddox et al. (3) in the rat.

arteriole) and that the early tubule is surrounded by small branch peritubular capillaries (3). Values assigned to efferent plasma were equivalent to those in Table I (PCO_2 = 55 mm Hg, C_{2b} = 29.3 mM), while concentrations in capillaries adjacent to early tubule segments were assumed to be elevated slightly (PCO_2 = 59 mm Hg, C_{2b} = 31.9 mM) consistent with available micropuncture data (14). When these inputs were used F_B and all concentrations both in the lumen and cell varied by <2% from their baseline values, throughout the tubule. This indicates that the normal gradients in PCO_2 and HCO_3^- concentration in the microvascular network surrounding the tubule have relatively little effect on events within the tubule.

For the model calculations we have assumed a volume flux or radial velocity at the brush border (v_m) which is constant with position. It has been observed, however, that the volume fluxes decrease along the tubule (3–5). A correlation between the fractional reabsorption rate of water (F_w) and both axial position (z) and *SNGFR* was derived from the data of Maddox and Gennari (4) using the same approach as that employed in obtaining Eq. 12. The functional form chosen was

$$F_w = \frac{z(1 + a_5 z)}{a_6 + a_7 SNGFR + a_8 SNGFR^2}. \qquad (15)$$

Using values of a_5 – a_8 of −0.083, 2.783, 0.127, and -1.05×10^{-3} (where z is in mm and *SNGFR* is in nl/min), respectively, yielded a very satisfactory fit to the data for *SNGFR* = 10–70 nl/min (RMS error = 0.05). Because $a_5 < 0$, Eq. 15 implies a linear decrease in v_m with z. When a linear function $v_m(z)$ consistent with the correlation in Eq. 15 was employed, F_B varied by <0.012 from the values represented in curve *E* of Fig. 1. Therefore, for all other calculations we utilized a value of v_m which was constant with position, but which varied with *SNGFR* to yield the fractional water reabsorption at z = 5 mm given by Eq. 15.

Thus far, the comparisons we have made with measured rates of bicarbonate reabsorption have been limited to a single filtered load. Fig. 7 compares the predicted and observed relationships between bicarbonate filtered load and absolute bicarbonate reabsorption up to the late proximal tubule (assumed to be at z = 5 mm). In obtaining the model predictions (solid curves) the filtered load was varied in two ways. The upper solid curve corresponds to variations in *SNGFR* with the HCO_3^- concentration in Bowman's space held constant, $C_2(0)$ = 30.8 mM. The lower curve was calculated by varying $C_2(0)$ with *SNGFR* held at 30 nl/min. It can be seen that the predicted rates of bicarbonate reabsorption (R_B) at a given filtered load (Λ) are quite similar, irrespective of how that filtered load was obtained. This prediction is consistent with most of the available micropuncture data in the rat, covering a wide range of experimental conditions. The data points in Fig. 7 represent mean values obtained from a number of studies,

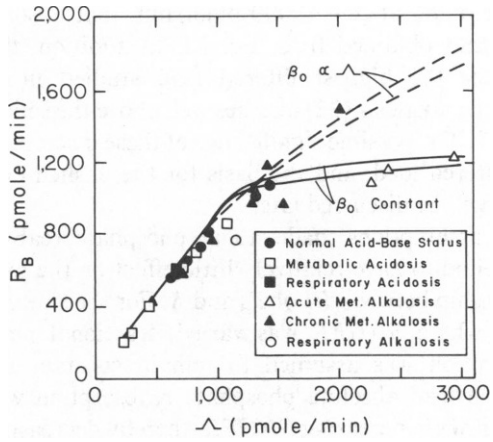

FIGURE 7 Predicted and observed dependence of absolute bicarbonate reabsorption (R_B) on bicarbonate filtered load (Λ). The solid curves are model predictions using the parameters in Table I, and assume that β_0 is constant. The dashed curves are model predictions assuming that $\beta_0 \propto \Lambda$. The upper curve in each pair is based on variable *SNGFR* with $C_2(0)$ = 30.8 mM; the lower curve in each pair assumes that *SNGFR* = 30 nl/min and $C_2(0)$ is variable. In all cases it is assumed that PCO_2 = 55 mm Hg in Bowman's space. The data points represent mean values selected from several free-flow micropuncture studies in the rat (5, 16–18, 20–22).

and include experimental periods where plasma pH and HCO_3^- concentration were within normal ranges (5, 16–18, 20) or were perturbed in several ways, including induction of metabolic acidosis (16, 17), respiratory acidosis (17) or alkalosis (18), and acute (18, 21) or chronic (18, 20–22) metabolic alkalosis. In several of these studies *SNGFR* was also varied, by means of maneuvers such as plasma volume expansion or aortic constriction. Although not shown, the standard errors of R_B and Λ in these micropuncture studies were typically 5–10% of the mean values. It can be seen that, with a few exceptions, the data are consistent with the concept of a unique relationship between R_B and Λ. Furthermore, the model predictions using the baseline parameters in Table I, shown by the solid curves in Fig. 7, are generally in excellent agreement with the data. In particular, the prediction of nearly constant values of R_B for Λ > 1400 pmol/min, corresponding to sharp declines in fractional HCO_3^- reabsorption, is remarkably consistent with measurements made by Cogan (18) and Cogan and Liu (21) in acute metabolic alkalosis.

Certain discrepancies between the model predictions and experimental observations may be quite significant, however. One major discrepancy involves the results obtained by varying *SNGFR* under normal acid-base conditions (4), data which are summarized as a correlation between F_B and Λ in Eq. 12. The simulations given by either solid curve in Fig. 7 agree very well with these micropuncture data for Λ < 1400 pmol/min, but the model significantly underestimates HCO_3^- reabsorption rates at higher filtered loads. Even the upper solid curve, which corresponds closely to the experimental conditions just described (*SNGFR* variable, $C_2(0)$ nearly constant), gives

a value of R_B at Λ = 2,000 pmol/min that is some 20% below that obtained from Eq. 12. In addition, the data point for the highest filtered load studied in chronic metabolic alkalosis (22) also lies well above the solid curves in Fig. 7. The possible significance of these discrepancies at high filtered load, and the basis for the dashed curves in Fig. 7, will be discussed later.

The assumptions made about phosphate reabsorption were found to have relatively little effect on the predicted relationship between R_B or F_B and Λ. For the simulation in Fig. 7 where *SNGFR* was varied, fractional phosphate reabsorption was assumed to remain constant at 60%. When instead absolute phosphate reabsorption was held constant with increasing *SNGFR*, thereby decreasing fractional phosphate reabsorption, F_B changed by <0.01.

Changes in absolute and fractional bicarbonate reabsorption are also predicted to occur at a fixed filtered load of bicarbonate, when PCO_2 is altered. When PCO_2 and pH were varied in such a way that HCO_3^- concentration in the filtrate was held constant, the results shown in Table III were obtained. Increasing PCO_2 lead to substantial increases in R_B, and hence F_B, under these circumstances. This was a result of perturbations in the calculated intracellular pH, secondary to changes in the pH of the filtrate and peritubular interstitium. Calculated values of intracellular pH (pH_c) along the proximal tubule ranged from 7.38 to 7.37 at PCO_2 = 30 mm Hg, and 7.15 to 7.00 at PCO_2 = 80 mm Hg. In interpreting these results, of course, the PCO_2 values given must be compared with the baseline value of 55 mm Hg in Bowman's space of superficial nephrons (3), rather than the normal PCO_2 of 40 mm Hg in the systemic circulation. These results appear to explain the unusually low fractional bicarbonate reabsorption rate that has been reported for respiratory alkalosis (18), which is in fact the data point in Fig. 7 which deviates most from the main pattern at low to moderate filtered loads. Increases in F_B or R_B in respiratory acidosis (17), relative to values at normal PCO_2 and comparable filtered loads, are difficult to detect in Fig. 7 because the fractional HCO_3^- reabsorption for normal systemic PCO_2 levels is already quite high. A more direct comparison of model predictions with micropuncture studies in respiratory alkalosis or acidosis would require measurements of PCO_2 in surface nephrons under these conditions, data which are not yet available.

TABLE III
EFFECT OF BOWMAN'S SPACE PCO_2 ON ABSOLUTE (R_B) AND FRACTIONAL (F_B) BICARBONATE REABSORPTION AT A FIXED FILTERED LOAD OF BICARBONATE*

PCO_2	R_B	F_B	pH_c
mmHg	*pmol/min*		
30	835	0.66	7.38–7.37
40	947	0.75	7.31–7.30
50	1037	0.82	7.26–7.23
60	1105	0.88	7.22–7.16
70	1152	0.92	7.18–7.08
80	1178	0.94	7.15–7.00

*In all of these calculations *SNGFR* = 40.8 nl/min and $C_2(0)$ = 30.8 mM, corresponding to Λ = 1,257 pmol/min.

The results of a study by Chan et al. (23), involving simultaneous tubule and peritubular capillary microperfusion, offer an additional opportunity to test the trends in bicarbonate reabsorption predicted by the present model. When bicarbonate concentrations were increased simultaneously in both perfusates, bicarbonate reabsorption was augmented, with greater increases seen when the perfusates were maintained at constant pH than at constant PCO_2. When bicarbonate load was varied by changing tubule perfusion rate (at constant composition), bicarbonate reabsorption changed less than when bicarbonate load was altered by changing tubule (and capillary) bicarbonate concentration, at constant pH. These trends are in qualitative agreement with the predictions of the model. The greater sensitivity of bicarbonate reabsorption to bicarbonate load seen when bicarbonate concentration and PCO_2 were allowed to change in parallel (constant pH of perfusates) can be understood as an effect of PCO_2 variations superimposed on those of variations in bicarbonate load. It should be noted, however, that in each case the experimental variations in bicarbonate reabsorption tended to be greater than those predicted by the model. For example, doubling bicarbonate concentration at constant pH was observed to increase bicarbonate reabsorption by a factor of 2.1, whereas our calculated increase was only a factor of 1.4. Quantitative comparisons are hampered by the fact that the lengths and locations of the perfused tubule segments were not reported by Chan et al. (23); we assumed a length of 1 mm beginning midway along the tubule. Furthermore, given the rapid diffusion of CO_2 across tubules and capillaries, it would appear questionable that the PCO_2 in these structures remained at the levels set in the perfusates, as assumed by Chan et al. (23). Even in their control conditions, the PCO_2 used was 40 mm Hg, well below that which has been measured in the superficial cortex under normal systemic acid-base conditions (3). For these reasons, it is not clear whether the quantitative discrepancies noted above are due to methodological difficulties, inadequacies of the model, or some combination of these.

DISCUSSION

Recent micropuncture measurements in the rat have demonstrated very convincingly that the local rate of bicarbonate reabsorption in the proximal convoluted tubule decreases markedly with increasing distance from Bowman's space (3–5). One of the objectives of the present study was to examine the extent to which this decline in HCO_3^- reabsorption flux (or H^+ secretory flux) could be explained by physical or chemical factors such as the declines in luminal flow rate and in luminal HCO_3^-

concentration and pH. Many of the pertinent physical and chemical phenomena were already embodied in the model of Wang and Deen (2), which included axial and radial variations in the concentrations of HCO_3^- and related chemical species in the tubule lumen and epithelial cells, and axial variations in luminal fluid velocity. However, as noted previously (2), that model included several simplifying assumptions which limit its applicability to very early segments of the proximal tubule. Accordingly, using the previous model as a starting point, a more complete description of events in the tubule lumen and epithelial cells was developed. Included specifically were several physiological factors which would be expected to progressively retard net bicarbonate reabsorption along the tubule. The added features include an expression for the H^+ flux that causes it to decrease as tubule fluid becomes more acidic (for a given intracellular pH), and allowances for buffering by luminal phosphate and for paracellular bicarbonate backleak. An important conclusion from the present work is that these factors are insufficient to explain the large decrease observed in bicarbonate fluxes along the tubule. To simulate the available data on axial variations in bicarbonate reabsorption rate it was necessary to postulate a decrease in the intrinsic reabsorptive capacity of the tubule with increasing distance from Bowman's space.

The principal parameters that describe reabsorptive capacity in the present formulation are the rate constant for H^+ secretion at the brush border membrane (β) and the effective HCO_3^- permeability at the basolateral membrane ($P_2[r_2]$). Excellent agreement with available micropuncture data was obtained when both of these membrane parameters were assumed to decrease exponentially with distance along the tubule, with the ratio of the initial (z = 0) to final (z = 5 mm) values being approximately 18. The progressive decreases in the apparent values of β and $P_2(r_2)$ could in part reflect decreases in the surface area per unit tubule length of the brush border and basolateral membranes, respectively. This is because all fluxes were expressed in terms of the surface areas of smooth cylinders of radii r_1 and r_2 enclosing the proximal epithelium, and effective membrane permeabilities in this model are therefore proportional to the ratio of the actual membrane surface area to the surface area of the corresponding ideal cylinders (2). Morphologic examination of cells from various segments of the proximal tubule has shown a simplification in membrane structure in later segments (24), suggesting that specific surface areas are in fact reduced. However, it is not clear that such reductions in specific surface area would be sufficient to fully explain the large decreases inferred for β and $P_2(r_2)$, leaving open the possibility of axial variations in the true membrane rate constants. It should be emphasized that while we chose to vary both parameters, axial variations in either β or $P_2(r_2)$, with the other quantity held constant, are sufficient to explain the micropuncture observations. Furthermore, in a limited examination of empirical functions other than the exponential forms used in Eqs. 13 and 14, we obtained equivalent results, provided that in the baseline case the axial variations in F_B were similar to the measured values summarized by Eq. 12. Although based on a different set of data and not expressed in terms of specific membrane parameters, a decline in bicarbonate reabsorptive capacity with distance along the tubule was also included in the model of Alpern and Rector (6).

As already mentioned in connection with Table II and Fig. 6, the values of β and $P_2(r_2)$ corresponding to our baseline case are reasonably consistent both with available data on intracellular pH in the rat proximal convoluted tubule (19), and with measurements of transepithelial differences in PCO_2 (3). However, in interpreting the values of these membrane parameters it should be kept in mind that the flux equations that define them (Eqs. 8 and 11) may be only qualitatively correct. Indeed, it is not certain that HCO_3^- per se is transported from the epithelial cell to the peritubular fluid, in that concurrent movement of CO_2 and OH^- would have the same net effect. Furthermore, diffusion of HCO_3^- across the brush border membrane was arbitrarily neglected in the present calculations ($P_2[r_1] = 0$); if this were included, the value of $P_2(r_2)$ would have to be increased at any given axial position, to compensate for the backleak of HCO_3^- from the cell to the tubule lumen that is predicted when $P_2(r_1) \neq 0$ (2). In view of the considerable uncertainties in β and $P_2(r_2)$, it is reassuring to note that any of several combinations of these parameters that gave the proper profile of HCO_3^- reabsorption rates for the reference conditions depicted in Fig. 3 ($SNGFR$ = 40.8 nl/min, $C_2(0)$ = 30.8 mM), also gave virtually identical predictions of HCO_3^- reabsorption under other conditions. Thus, uncertainties in these membrane parameters fortunately do not preclude the use of the model to examine the response of the tubule to variations in the filtered load of HCO_3^-.

For euvolemic Munich-Wistar rats with normal values of pH and HCO_3^- concentration in systemic plasma, the filtered load of HCO_3^- in a superficial nephron is typically ~1,200 pmol/min (3, 4). As shown in Fig. 7, the observed relationship between HCO_3^- reabsorption rate in the accessible proximal tubule (R_B) and filtered load (Λ) for $200 < \Lambda < 1{,}400$ pmol/min has been found to be quite similar, irrespective of how filtered load was varied. The findings for a variety of systemic acid-base states and $SNGFR$ values have been remarkably consistent when limited to this range of filtered loads, including data for rats where metabolic alkalosis was maintained up to ~2 wk, a condition of sufficient duration to be termed "chronic" (18, 20, 21). The predicted values of R_B for this range of Λ are also insensitive to whether filtered load is changed by varying $SNGFR$ or by varying HCO_3^- concentration in the filtrate (at constant PCO_2), and are generally quite close to the observed values.

At the high filtered loads ($\Lambda > 1{,}400$ pmol/min) achieved experimentally by marked elevation in $SNGFR$

or by the induction of metabolic alkalosis, the behavior of the proximal tubule is more difficult to explain. The model predictions for Λ as large as 2,200–3,000 pmol/min are in excellent agreement with the measurements of Cogan (18) and Cogan and Liu (21) in rats with acute metabolic alkalosis. In those studies mean *SNGFR* values (46–50 nl/min) were only slightly above our reference value of 41 nl/min, chosen to represent euvolemic Wistar rats. When high filtered loads were achieved in a relatively long-term metabolic alkalosis (2–4 wk, $\Lambda \simeq 2{,}000$ pmol/min) (22) or by acute elevations in *SNGFR* up to as high as 70 nl/min (4), however, the observed values of R_B greatly exceed those predicted by the model. The apparent enhancement of HCO_3^- reabsorptive capacity at high filtered loads either in chronic metabolic alkalosis or at very high *SNGFR* suggests an adaptive response by the tubule. In chronic metabolic alkalosis of 2–4 wk duration the length of the proximal tubule was found to average some 7 mm (Maddox and Gennari, personal communication), as compared with 5 mm in normal animals, a reflection of kidney growth. To compensate for this, the value of R_B shown in Fig. 7 for this study (1,500 pmol/min) is based on a length of 5 mm. Therefore, this high value of R_B appears to reflect some other adaptation, one which increases the reabsorptive capacity of a given length of tubule for HCO_3^-.

Of interest is the observation of Harris et al. (25) that the activity of the Na^+/H^+ exchanger (expressed per gram of membrane protein) in vesicles prepared from proximal brush border membranes was elevated in rats in which whole kidney GFR had been increased chronically (usually 2–3 wk) prior to sacrifice. Exchanger activity, corresponding most directly to the parameter β in the present model, appeared to increase in direct proportion to GFR. If β is assumed to vary directly with filtered load (with the reference values given in Table I), the model predictions are as shown by the dashed curves in Fig. 7. The upper dashed curve corresponds to variations in Λ at constant HCO_3^- concentration, while the lower curve is based on constant *SNGFR*. As can be seen, the predicted values of R_B for $\Lambda < 1{,}400$ pmol/min are virtually the same whether or not β is assumed to vary with Λ, but at higher filtered loads the values of R_B are significantly elevated when β is increased with Λ. The upper dashed curve in Fig. 7 is virtually identical to a plot of Eq. 12, which summarizes the experimental results of Maddox and Gennari (4) based on variations in *SNGFR*. The model prediction with $\beta \propto \Lambda$ is also in close accord with the data point corresponding to the highest filtered load studied in chronic metabolic alkalosis (22).

Increases in β stimulated by chronic elevations in filtered load provide an attractive explanation for the different reabsorptive capacities for HCO_3^- in chronic (22) as compared with acute (18, 21) metabolic alkalosis. In the vesicle transport studies mentioned above (25) an increase in Na^+/H^+ exchanger activity was evident as soon as one day after contralateral nephrectomy, a maneuver used to increase *SNGFR* in remaining nephrons. However, to explain the very high values of R_B seen with large, acute elevations in *SNGFR* (4), the postulated increase in β would have to occur within ~1 h. We are not aware of any independent evidence (e.g. from vesicle studies) for an adaptive response in H^+ secretion on this short a time scale. Experiments which address this possibility would clearly be of interest.

We have attempted without success to identify a purely physical basis for the apparent dependence of HCO_3^- reabsorptive capacity on *SNGFR*. One possibility considered was that the increased luminal pressures associated with elevated *SNGFR* might somehow enhance HCO_3^- reabsorption by increasing the tubule radius. This situation was simulated by letting the luminal radius (r_1) vary according to the compliance measurements of Cortell et al. (26), while either cell volume or thickness (r_2–r_1) were held constant. Because of the highly folded nature of the cell membranes, the membrane permeability parameters (corrected for membrane surface area) were assumed to be independent of r_1 and r_2. No significant effect on HCO_3^- reabsorption was seen.

Another possible physical explanation for flow-dependence of HCO_3^- reabsorption has been advanced by Alpern et al. (27). By varying the perfusion rate of rat proximal tubules in vivo, these authors were able to demonstrate substantial increases in HCO_3^- reabsorption with luminal flow. The measured increases greatly exceeded those expected simply from the effect of flow on axial variations in HCO_3^- concentration. They found their results to be most consistent with the concept of a flow-dependent luminal diffusion barrier or unstirred layer for HCO_3^-. We find this explanation to be unconvincing for two reasons. First, radial concentration variations in the tubule lumen were included for all chemical species in the present model as well as in the previous study by Wang and Deen (2), and were calculated to be small except during simulated inhibition of carbonic anhydrase (2). More importantly perhaps, even if luminal mass transfer resistances were *not* small, there is little reason to expect them to be affected by axial velocity. As discussed previously (2), in a permeable cylindrical tube having the flow rates and dimensions of the proximal tubule, the radial variations in axial velocity and in solute concentrations within the lumen are expected to achieve a "fully developed" character within at most a few radii downstream from the inlet (corresponding to Bowman's space or to a perfusion pipette). When flow is laminar and velocity and concentration profiles are fully developed throughout most of the length of a tube, it is well established that mass transfer coefficients (or the analogous heat transfer coefficients) are independent of axial fluid velocity (28, 29). This conclusion holds not only for cylindrical tubes but also for channels with other cross-sectional shapes, and for a variety of mass transfer boundary conditions at the tube wall.

The conclusion that changes in luminal velocity do not affect mass transfer coefficients, for hydrodynamic conditions representative of the proximal tubule, applies strictly only to channels with smooth walls. The brush border membrane of the proximal tubule contains of course numerous microvilli, raising the question of whether changes in axial velocity might enhance mass transfer in this region. The characteristics of viscous flow through structures of this type were investigated by Basmadjian et al. (30) using a combination of fabricated experimental models and theoretical analysis. Those authors estimated that, depending on the geometrical details assumed for the brush border, the axial fluid velocity (U) in that region should range from about 3×10^{-6} to 4×10^{-4} cm/s, at a total flow rate of 20 nl/min. From these results we can readily calculate a Peclet number (Pe) for the interstices of the brush border, a dimensionless group which measures the relative effects of convection and diffusion on solute transport. Choosing the length of a microvillus as the characteristic dimension ($L \simeq 3$ μm) and $D = 10^{-5}$ cm^2/s as a typical diffusivity, we obtain $Pe = UL/D = 10^{-4}$ to 10^{-2} from the range of velocities given above. This indicates that even if the mass transfer resistance in this region were large enough to significantly affect HCO_3^- reabsorption, a point which has not been established, solute concentration profiles would not be altered significantly by variations in axial flow. Similar conclusions were reached by Basmadjian et al. (30), who also argued against the possibility of appreciable mass transfer enhancement by motion of the microvilli. We conclude that while there is substantial experimental evidence in vivo for a dependence of bicarbonate reabsorptive capacity on luminal flow, there is at present no adequate physical explanation for this phenomenon. This issue certainly deserves further study.

An important feature of the present model is its provision of a mechanism by which intracellular pH can respond to changes in the pH and PCO_2 of tubule fluid and peritubular plasma. This allowed predictions of the effects of PCO_2 on bicarbonate reabsorption, with results (Table III) generally similar to those seen after induction of respiratory alkalosis (18) or acidosis (17), or following variations in bath PCO_2 with isolated perfused tubules (31). Intracellular pH was coupled to H^+ and HCO_3^- transport, and therefore to the extracellular fluid compositions, largely through Eqs. 8–11. The form of the expression for the H^+ secretion rate (Eq. 8) approximates the kinetics of Na^+/H^+ exchange revealed by studies using brush border membrane vesicles, although the observed dependence of flux on intracellular H^+ concentration is not exactly linear (32). Perhaps more problematic are the assumptions that H^+ transport is confined to the brush border membrane (Eq. 9), and that HCO_3^- movement across the basolateral membrane follows the simple rate law given by Eq. 11. It is likely that some or all of these flux expressions will need to be modified as more is learned about the rates of H^+ and HCO_3^- transport. A more realistic model may need to recognize explicitly the coupled transport of these substances with Na^+ or other ions (33), and the factors governing intracellular potential. We hope that the present model will provide a suitable framework for adding these refinements.

The authors are grateful for many helpful discussions with Drs. D. A. Maddox and F. J. Gennari during the course of this work, including access to some of their unpublished data. Drs. R. J. Alpern, M. G. Cogan, and F. C. Rector, Jr. were also kind enough to alert us to some of their recent experimental results, and in doing so have helped make this study more complete. The authors also acknowledge the expert assistance in manuscript preparation provided by Glorianne Collver-Jacobson.

This work was supported by a grant from the National Institutes of Health (AM 20368). L. J. Atherton is the recipient of a predoctoral fellowship from the Whitaker Health Sciences Fund.

Received for publication 21 May 1985 and in final form 21 February 1986.

REFERENCES

1. Warnock, D. G., and F. C. Rector, Jr. 1981. Renal acidification mechanisms. *In* The Kidney. Second Edition. B. M. Brenner and F. C. Rector, Jr., editors. W. B. Saunders Co., New York. p. 440.
2. Wang, K. W., and W. M. Deen. 1980. Chemical kinetic and diffusional limitations on bicarbonate reabsorption by the proximal tubule. *Biophys. J.* 31:161.
3. Maddox, D. A., L. J. Atherton, W. M. Deen, and F. J. Gennari. 1984. Proximal HCO_3^- reabsorption and the determinants of tubular and capillary PCO_2 in the rat. *Am. J. Physiol.* 247:F73.
4. Maddox, D. A., and F. J. Gennari. 1985. Load dependence of HCO_3^- and H_2O reabsorption in the early proximal tubule of the Munich-Wistar rat. *Am. J. Physiol.* 248:F113.
5. Liu, F.-Y., and M. G. Cogan. 1984. Axial heterogeneity in the rat proximal convoluted tubule. I. Bicarbonate, chloride, and water transport. *Am. J. Physiol.* 247:F816.
6. Alpern, R. J., and F. C. Rector, Jr. 1985. A model of proximal tubular bicarbonate absorption. *Am. J. Physiol.* 248:F272.
7. Gros, G., W. Moll, H. Hoppe, and H. Gros. 1976. Proton transport by phosphate diffusion. A mechanism of facilitated CO_2 transfer. *J. Gen. Physiol.* 67:773.
8. Macey, R. I. 1963. Pressure flow patterns in a cylinder with reabsorbing walls. *Bull. Math. Biophys.* 25:1.
9. Alpern, R. J., M. G. Cogan, and F. C. Rector, Jr. 1983. Effects of extracellular fluid volume and plasma bicarbonate concentration on proximal acidification in the rat. *J. Clin. Invest.* 71:736.
10. Goldman, D. E. 1943. Potential, impedance, and rectification in membranes. *J. Gen. Physiol.* 27:37.
11. Gros, G., and W. Moll. 1974. Facilitated diffusion of CO_2 across albumin solutions. *J. Gen. Physiol.* 64:356.
12. Alpern, R. J., M. G. Cogan, and F. C. Rector, Jr. 1982. Effect of luminal bicarbonate concentration on proximal acidification in the rat. *Am. J. Physiol.* 243:F53.
13. Maren, T. H. 1978. Carbon dioxide equilibria in the kidney: the problems of elevated carbon dioxide tension, delayed dehydration, and disequilibrium pH. *Kidney Int.* 14:395.
14. Atherton, L. J., W. M. Deen, D. A. Maddox, and F. J. Gennari. 1984. Analysis of the factors influencing peritubular PCO_2 in the rat. *Am. J. Physiol.* 247:F61.
15. Greger, R., F. Lang, G. Marchand, and F. G. Knox. 1977. Site of renal phosphate reabsorption. Micropuncture and microinfusion study. *Pfluegers Arch. Eur. J. Physiol.* 369:111.
16. Cogan, M. G., D. A. Maddox, M. S. Lucci, and F. C. Rector, Jr. 1979. Control of proximal bicarbonate reabsorption in normal and acidotic rats. *J. Clin. Invest.* 64:1168.

17. Cogan, M. G., and F. C. Rector, Jr. 1982. Proximal reabsorption during metabolic acidosis in the rat. *Am. J. Physiol.* 242:F499.
18. Cogan, M. G. 1984. Effects of acute alterations in PCO_2 on proximal HCO_3^-, Cl^-, and H_2O reabsorption. *Am. J. Physiol.* 246:F21.
19. Yoshitomi, K., and E. Fromter. 1984. The intracellular pH of rat kidney proximal tubular cells in vivo. *IXth Intern. Congr. Neph.* 390A. (Abstr.)
20. Maddox, D. A., and F. J. Gennari. 1983. Proximal tubular bicarbonate reabsorption and PCO_2 in chronic metabolic alkalosis in the rat. *J. Clin. Invest.* 72:1385.
21. Cogan, M. G., and F.-Y. Liu. 1983. Metabolic alkalosis in the rat. *J. Clin. Invest.* 71:1141.
22. Maddox, D. A., and F. J. Gennari. 1985. Proximal HCO_3 reabsorption in chronic metabolic alkalosis in the rat. *Clin. Res.* 33:492A. (Abstr.)
23. Chan, Y. L., B. Biagi, and G. Giebisch. 1982. Control mechanisms of bicarbonate transport across the rat proximal convoluted tubule. *Am. J. Physiol.* 242:F532.
24. Maunsbach, A. B. 1973. Ultrastructure of the proximal tubule. *In* Handbook of Physiology: Renal Physiology. J. W. Orloff and R. W. Berliner, editors. *Am. Physiol. Soc. Wash.* D.C. 31.
25. Harris, R. C., J. L. Seifter, and B. M. Brenner. 1984. Adaptation of Na^+-H^+ exchange in renal microvillus membrane vesicles. *J. Clin. Invest.* 74:1979.
26. Cortell, S., F. J. Gennari, M. Davidman, W. H. Bossert, and W. B. Schwartz. 1973. A definition of proximal and distal tubular compliance. *J. Clin. Invest.* 52:2330.
27. Alpern, R. J., M. G. Cogan, and F. C. Rector, Jr. 1983. Flow dependence of proximal tubular bicarbonate absorption. *Am. J. Physiol.* 245:F478.
28. Shah, R. K., and A. L. London, 1978. Laminar Flow Forced Convection in Ducts. Advances in Heat Transfer. Academic Press, Inc. New York.
29. Colton, C. K., K. A. Smith, P. Stroeve, and E. W. Merrill, 1971. Laminar flow mass transfer in a flat duct with permeable walls. *AIChE J.* 17:773.
30. Basmadjian, D., D. S. Dykes, and A. D. Baines. 1980. Flow through brush-borders and similar protuberant wall structures. *J. Membr. Biol.* 56:183.
31. Jacobson, H. R. 1981. Effects of CO_2 and acetazolamide on bicarbonate and fluid transport in rabbit proximal tubules. *Am. J. Physiol.* 240:F54.
32. Aronson, P. S., J. Nee, and M. A. Suhm. 1982. Modifier role of internal H^+ in activating the Na^+-H^+ exchanger in renal microvillus membrane vesicles. *Nature (Lond.).* 299:161.
33. Boron, W. F., and E. L. Boulpaep. 1983. Intracellular pH regulation in the renal proximal tubule of the salamander. Basolateral HCO_3^- transport. *J. Gen. Physiol.* 81:53.